Hybrid Methods in Designing Sierpinski Gasket Antennas

Mudrik Alaydrus
Department of Electrical Engineering, University of Mercu Buana,
Jalan Meruya Raya Selatan, Jakarta, 11650, Ph: +62 21 28041003
e-mail: mudrikalaydrus@mercubuana.ac.id

Abstrak

Antena Sierpinski gasket sebagai sebuah contoh dari kelompok antena fraktal menunjukkan karakter pita jamak. Simulasi dengan komputer dari sebuah antena kutub tunggal Sierpinski gasket membutuh memori komputer yang besar dan waktu perhitungan yang lama. Metoda hybrid yang terdiri dari metoda persamaan integral permukaan dan optik fisika atau teori difraksi geometri seragam bisa melewati halangan komputasi ini. Hibridisasi penuh dengan memodifikasi gelombang elektromagnetika yang datang pada kasus metoda hybrid persamaan integral dan optik fisika atau modifikasi fungsi Green pada kasus metoda hybrid persamaan integral dan teori difraksi geometri seragam memainkan peran utama pada pengamatan di sini. Perbandingan hasil-hasil yang didapat dengan metoda-metoda ini akan diberikan juga dengan hasil pengukuran di lapangan terhadap tiga antena Sierpinski gasket. Karakter pita jamak masih terlihat, walaupun resonansi yang terjadi membesar dan mengecil.

Kata kunci: antena fractal, difraksi, komputasi, metoda persamaan integral, Sierpinski gasket

Abstract

Sierpinki gasket antennas as example of fractal antennas show multiband characteristics. The computer simulation of Sierpinksi gasket monopole with finite ground needs prohibitively large computer memory and computational time. Hybrid methods consist of surface integral equation method and physical optics or uniform geometrical theory of diffraction is expected to alleviate this computational burdens. The full hybridization of the different methods with modifying the incoming electromagnetic waves in case of hybrid method surface integral equation method and physical optics and modification of the Greens function for hybrid method surface integral equation method and uniform geometrical theory of diffraction plays the central role in the observation. A comparison of simulation results of these different methods and are given measurements of a groups of three Sierpinksi gasket antennas are presented. The multiband characteristics of the antennas are observed with some reduction and enhancement of resonances.

Keywords: computation, diffraction, fractal antenna, integral equation method, Sierpinski gasket

1. Introduction

The fast transmission of data in today communication systems requires a reliable and stable communication link between transmitter and receiver. Antennas as a part of this communication link can decide the success of this target. The demand on high performance wireless communication systems presupposes high performance antenna capabilities too. In designing of antennas, it is faced with several important quantities which must be fulfilled for each specific application. These antenna characteristics are return loss, radiation diagram, and gain. They must conform with certain specifications given to the antenna designer.

In order to meet the specifications, many new antennas are designed. Sierpinski gasket antenna which belongs to the group of fractal antennas is an example. Puente-Baliarda et al [1] reported the multiband characteristics of fractal Sierpinski antennas. The Sierpinski gasket is constructed by subtracting a central inverted triangle from a main triangle shape. One can iterate the same subtraction procedure on the remaining triangles.

In the recent times there are numerous investigations, for example [2], [3], [4], [5], are performed to improve the reflection characteristics of the Sierpinski gasket antennas and to change the positions of the resonances (conditions with minimal reflections). In these investigations the researcher perturbed the self-similarity of the Sierpinski fractal structure. In [6] a three dimensional conical antenna is analyzed. This antenna is build by wrapping a modified Sierpinski gasket. The result gives an increase in the impedance bandwidth and improvement of the radiation diagram performance. Alaydrus [7] extends the observation of Sierpinski gasket antennas to its three dimensional version, he showed, the operating bandwidth of the antenna is widened.

In all of the works mentioned before, the theoretical approach is made by use of numerical methods based on surface integral equation method (SIEM), finite difference time domain (FDTD) or finite element method (FEM). These numerical methods belong to exact calculation methods [8]. The word exact should be understood, that the derivation of the methods from the Maxwell's equations to special expressions in each method is carried out without any approximations. The common character of these methods is the large demand on computer memory if the structures under consideration are large compared to the wavelength. This condition is met, if the finite metallic ground beneath the antenna must be taken into account during the calculation.

In this work, two hybrid methods based on combination between surface integral equation method (SIEM) and two high frequency methods, the physical optics (PO) and the uniform geometrical theory of diffraction (UTD) are applied. PO and UTD are approximated methods, which become better, the larger the structures compared to the wavelength. In implementing SIEM+PO, the dimension of the system matrix does not affected by the extent of the PO structures, which leads to small computer memory requirement and short computational time. It just needs to compute additional integrals. In SIEM+UTD, it does not need even any integration on the UTD structures, so that, the hybrid methods provide a very efficient alternative to solve scattering problems consisting of electrically large structures. The software is developed in GNU C.

In section 2, some fundamental things of three methods, SIEM, PO and UTD are described separately. The combination of SIEM with PO and SIEM with UTD is explained in section 3, especially where the interface is done. Some calculation results concerning Sierpinski gasket antennas will be shown in section 4, and are compared with measurements.

2. Numerical Methods
2.1. Surface Integral Equation Method (SIEM)

In solving many antennas and scattering problems, the integral equation method shows its superiority in the direct fulfilling of the radiation boundary condition [9], [10]. This boundary condition is inherently included in the kernel of the integrals, the Green functions. There are several formulations for Green functions derived for different environments. In this work, the perfectly conducting metallic antenna structures located in free space are the main focus. For solving such structures it is advantageous to use the surface integral equation method (SIEM). SIEM used in this paper begins with the formulation of electric field in an arbitrary observation point r through integration of the electric current density $\vec{J}_S(\vec{r}')$ flowing on the surface of metallic structures S,

$$\vec{E}(\vec{r}) = -j\omega \iint_S G(\vec{r},\vec{r}') \cdot \vec{J}_S(\vec{r}')dS' - \frac{j}{\omega \varepsilon_o \mu_o} \nabla \left(\nabla \cdot \iint_S G(\vec{r},\vec{r}') \cdot \vec{J}_S(\vec{r}')dS' \right) \tag{1}$$

$\omega = 2\pi f$ is the radian frequency; ε_o and μ_o are permittivity and permeability of the free space, respectively. $G(\vec{r},\vec{r}')$ is the Green function in free space, which given by

$$G(\vec{r},\vec{r}') = \frac{\mu_o}{4\pi} \frac{e^{-jk|\vec{r}-\vec{r}'|}}{|\vec{r}-\vec{r}'|} \tag{2}$$

k is the wave number.

The calculation of the integrals in equation (1) is a computer-intensive process; however, more challenging is the determination of the up to now still unknown distribution of the the electric current density. This is the core of the SIEM. In literature, there are three different formulations used to solve the problems by means of SIEM. They are the electric field integral equation (EFIE), the magnetic field integral equation (MFIE) and the combined field integral equation (CFIE) [9], [10]. In EFIE, the requirement, that the tangential component of the electric field on ideally conducting surface must vanish, leads to the following integral equation

$$\hat{n} \times \left(-j\omega \iint_S G(\vec{r},\vec{r}') \cdot \vec{J}_S(\vec{r}')dS' - \frac{j}{\omega \varepsilon_o \mu_o} \nabla \left(\nabla \cdot \iint_S G(\vec{r},\vec{r}') \cdot \vec{J}_S(\vec{r}')dS' \right) + \vec{E}^{inc}(\vec{r}) \right) = 0 \quad (3)$$

The surface electric current flowing on the metallic structures can show complicated distribution. In the earlier time, the researchers tried to use some complex function to describe the electric current. Now, almost all problems are tackled by discretizing the structures into small elements, here triangles (as shown in Figure 1), so that the current density is described by certain simple basis functions, with *n* unknown amplitudes on each triangle (or on edges of the triangles). The most widely used basis functions are triangular Rao-Wilton-Glisson (RWG) vector basis function [10], which is just a linear function. It is distinguished between external and internal edges. In the RWG formulation, only internal edges are taken into account as unknown amplitudes.
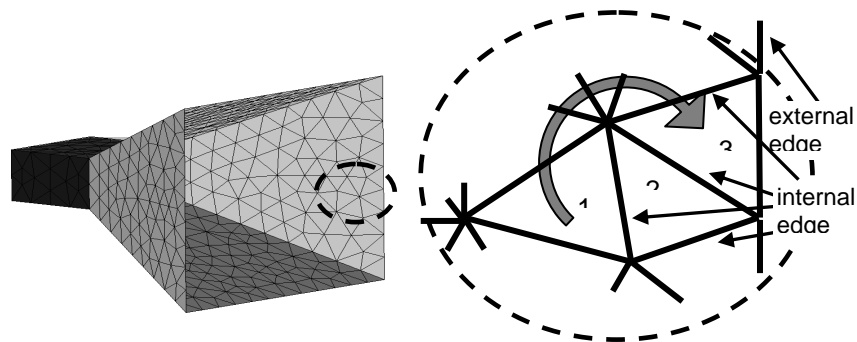

Figure 1. Discretization of a horn antenna into small triangles.

In order to solve the equation consisting *n* variables, it is applied the method of moment by means of Galerkin procedure, which results in a system of linear equations. The elements of the matrix in this linear system describe the mutual coupling of each element. Figure 1 shows a coupling between element 1 and 3.

The solution of this matrix problem gives us the amplitudes of the basis functions, so that the current on the radiating structures is determined. Other antenna characteristics, like input impedance, radiation diagram can be calculated with these current densities.

2.2. Uniform Geometrical Theory of Diffraction (UTD)
The basis of uniform geometrical theory of diffraction (UTD) is geometrical optics (GO). In this theory, the complex mechanism of scattering into separate simpler mechanism, like direct propagation, reflections, diffractions, and combined mechanisms is subdivided. Figure 2 shows a source of electromagnetic waves located in free space, and there are several structures in the vicinity. Observation of the waves in any point in the region leads to superposition of any possible contributions from the source, scattered by the structures, and received in the observation point.

In geometrical optics, the propagation of electromagnetic waves is governed by the Fermat's law. The Fermat's law states, the waves take the propagation path that can be passed in shortest time. In homogeneous region, the propagation path is a line. The change of propagation path due to reflection of waves on structures, and also diffraction at a boundary of a

structure, follows this law too. So that, the process of ray tracing can be performed by following the Fermat's law. The second important law in GO is the law of the conservation of the energy.
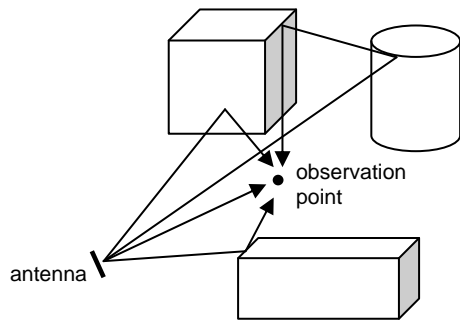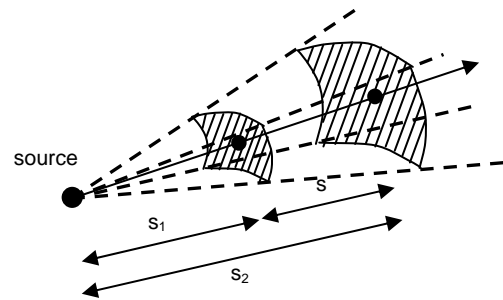

Figure 2. Scattering mechanisms in UTD

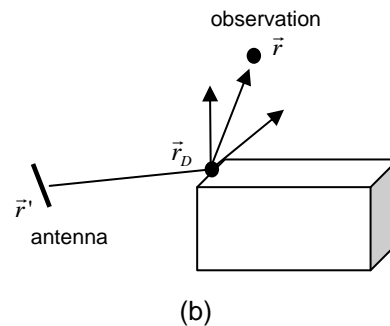Figure 3. Ray tube ensuring energy conservation
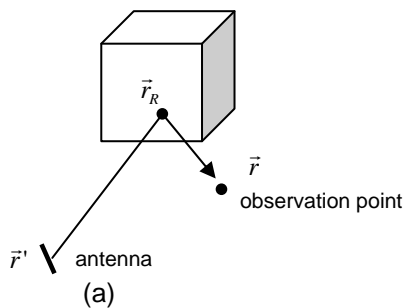

(a)

(b)

Figure 4. Visualization of the two mechanisms in UTD (a) reflection on a plane,
(b) diffraction at an edge

Figure 3 shows a ray tube as the model for wave propagation in GO. The direction of ray or propagation is designated by the arrow; it is a line in homogeneous media. The energy is confined inside the tube, i.e. the electromagnetic energy through the shaded areas in Figure 3 is the same. In the case the wave diverges, the shaded area A_2 is bigger than A_1, the Poynting vector S on A_2 is consequently smaller than on A_1. With this consideration, the electric field at distance s from a certain reference point s_1, can be calculated with the equation (4)

$$\vec{E}(s_2 = s_1 + s) = \vec{E}(s_1) \cdot \frac{s_1}{s_1 + s} \cdot e^{-jks} \tag{4}$$

The expression in the equation (4) is included in the far-field calculation of any kind of antennas.

Figure 4 visualizes the two other single important mechanisms in UTD. Figure 4a gives information about reflected wave on a wall or plane at the point $\vec{r}_R$. The exact position of reflection point $\vec{r}_R$ can be localized by ray tracing process. The reflected electric field at the observation point can be then determined by equation (5)

$$\vec{E}(\vec{r}) = \vec{R} \cdot \vec{E}(\vec{r}_R) \cdot \frac{s_1}{s_1 + s} \cdot e^{-jks} \tag{5}$$

s_1 and s are distances between antenna and reflection point, and between reflection point and observation point, respectively. $\vec{R}$ is the dyadic reflection coefficient. The reflection coefficient of ideally conducting metallic plane is +1 and -1 for parallel and perpendicular polarization, respectively. The dyadic coefficient can be calculated with respect to the orientation of the plane.

Whereas, Figure 4b shows the diffraction of waves at an edge of a plane. If an incident wave hits an edge, diffracted waves emerges. Just a diffracted wave will reach the observation point $\vec{r}$. Again, the exact position of the diffraction point $\vec{r}_D$ can be determined by ray tracing process. The diffracted electric field can be then calculated by

$$\vec{E}(\vec{r}) = \vec{D} \cdot \vec{E}(\vec{r}_D) \cdot \sqrt{\frac{s_1}{s \cdot (s_1 + s)}} \cdot e^{-jks} \qquad (6)$$

$\vec{D}$ is the dyadic diffraction coefficient. The detail calculation of this coefficient documented very well in [11].

2.3. Physical Optics (PO)
The scenario in Figure 2 can be recalled here. The antenna radiates electromagnetic waves in its environment. The waves illuminate some of the structures. The others are not directly, because of shadowing by another structure. The physical optics (PO) makes use also the equation (1) for calculating the electric field like in SIEM. The integration is indeed the most time-consuming process in PO. If the distance from the structure to the observation point is large, sometimes the far-field approach is used. It can reduce the calculation complexity. The fundamental distinction between PO and SIEM is, in SIEM the current distribution is unknown; in PO it is can be approximated the current distribution on the scattering structures by physical optical approach [12].

$$\vec{J}_{S,PO}(\vec{r}) = \begin{cases} 2\,\hat{n} \times \vec{H}^{inc}(\vec{r}) & \text{lit region} \\ 0 & \text{shadow region} \end{cases} \qquad (7)$$

$\hat{n}$ is the normal vector of the scattering structure and $\vec{H}^{inc}$ is any incident magnetic field produced by the antenna. As equation (7) states, only lit structures can radiate electromagnetic fields. Therefore, it is very important to know, whether the structures under consideration are shadowed or not.

3. Hybrid Method
SIEM is in respect to the modeling certainly an exact method. The results obtained by SIEM represent thrustworthy data. However, as mentioned in the previous section, if the structures under consideration are large enough compared to the wavelength, the computational effort, i.e. the memory requirement and the computing time, becomes prohibitively large. In this work it is used the calculation results obtained by SIEM as reference.
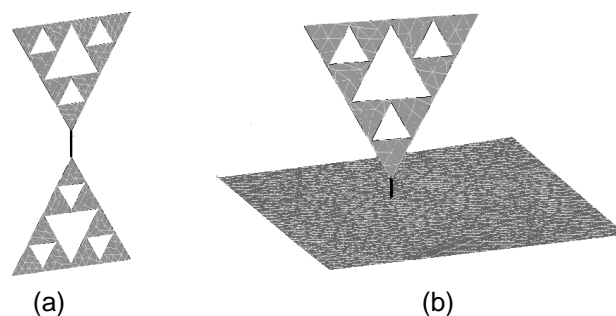

(a) (b)

Figure 5 (a) Sierpinksi gasket fractal antena dipole (third iteration),
(b) Sierpinski gasket fractal antena monopole with finite ground

Figure 5a and 5b show the Sierpinski gasket antenna of third iteration with dipole version and monopole version, respectively. In this work it is make computer calculations for both versions, however just the monopoles are built as prototypes. In calculation, the dipoles

are computed with SIEM, and the monopoles are modeled by SIEM, hybrid method SIEM+UTD and hybrid method SIEM+PO.

3.1. Hybridization of SIEM and PO (SIEM+PO)

The most important equation in SIEM is equation (3). This equation describes explicitly the coupling mechanisms between each element. This interaction shapes the current distribution in one or another way. Because the interaction occurs between all elements, the matrix obtained by SIEM is a fully occupied one. The existence of large structure, in case the finite ground of the antenna, will be taken into account with PO, so that the ground is designated as PO structure.

The SIEM structure generates electromagnetic waves as states in equation (1), the electromagnetic waves induce electric current density on the PO structure. This induced current density generates in turn electromagnetic waves. The electromagnetic waves produced by PO structure considered as incident waves in equation (3). The couping mechanism between SIEM and PO is visualized in Figure 6 [13].

Generation of $\vec{E}^{inc}$ (equation 1), calculation of $\vec{H}^{inc}$ (Maxwell equations), calculation $\vec{J}_{S,PO}$ (equation 7)

SIEM

PO structure

With $\vec{J}_{S,PO}$, calculation $\vec{E}$, using this electric field as incident wave $\vec{E}^{inc}$ in equation 3
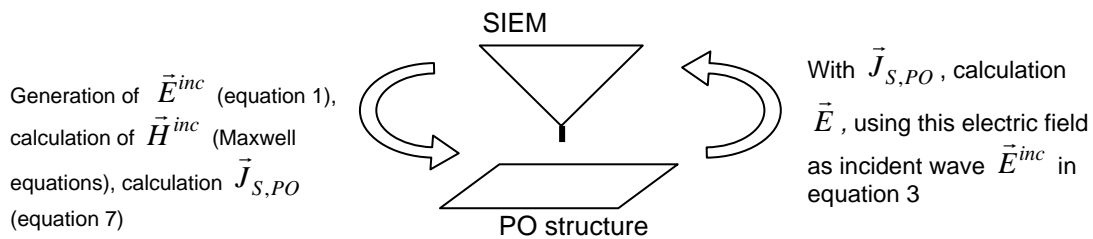
Figure 6 Coupling in hybrid method SIEM+PO

In this way, the presence of the PO structure modifies the elements of the matrix. The dimension of the matrix self is unchanged.

3.2. Hybridization of SIEM and UTD (SIEM+UTD)

As described in section 2, UTD does not need any integration. Any available incoming electromagnetic waves can be reflected and diffracted. Figure 7 visualized the condition in coupling between elements in the hybrid method SIEM+UTD. Not only direct coupling between the elements exists, as described in equation (3), it is observed also coupling via reflections on planes and diffractions at edges of UTD structures.

Each element radiates electromagnetic waves into space. The waves reach the mutual element directly (a) or via a reflection (b) and diffraction (c)

(a)

SIEM

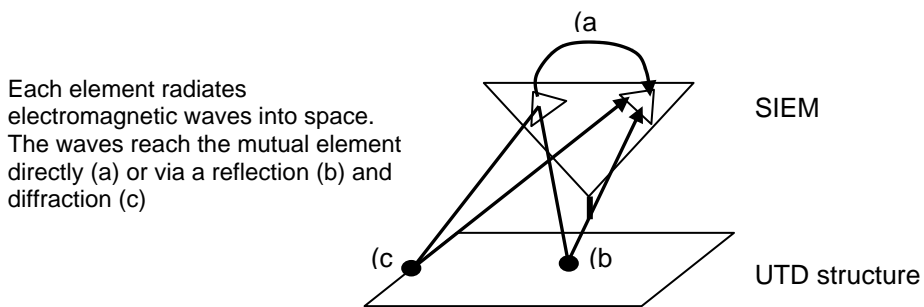(c)   (b)

UTD structure

Figure 7 Coupling in hybrid method SIEM+UTD

Mathematically, it must be modified the Green function used in equation (3), to the dyadic Green function

$$\ddot{G}_{\mathrm{mod}}\left(\vec{r},\vec{r}'\right) = \ddot{I}G\left(\vec{r},\vec{r}'\right) + \sum \ddot{G}_{ref}\left(\vec{r},\vec{r}',\vec{r}_R\right) + \sum \ddot{G}_{dif}\left(\vec{r},\vec{r}',\vec{r}_D\right) + \cdots \qquad (8)$$

$G(\vec{r}, \vec{r}')$ is the Green function in empty free space as introduced in equation (2) with the unit dyadic $\vec{I}$. $\vec{G}_{ref}(\vec{r}, \vec{r}', \vec{r}_R)$ is the additional Green function due to reflection [14], which stated as

$$G_{ref}(\vec{r}, \vec{r}', \vec{r}_R) = \vec{R} \cdot \vec{I} \cdot G(\vec{r}_R, \vec{r}') \cdot \frac{s_1}{s_1 + s} \cdot e^{-jks} \tag{9}$$

And $\vec{G}_{dif}(\vec{r}, \vec{r}', \vec{r}_D)$ for diffraction

$$\vec{G}_{dif}(\vec{r}, \vec{r}', \vec{r}_D) = \vec{D} \cdot \vec{I} \cdot G(\vec{r}_D, \vec{r}') \cdot \sqrt{\frac{s_1}{s(s_1 + s)}} \cdot e^{-jks} \tag{10}$$

Equation (8) considers also higher order mechanisms like double reflections, double diffractions, reflection followed by diffraction and so on [15].

The modified Green functions in equation (3) changes the element of the system matrix and shapes certain current distribution on the SIEM structure.

4. Calculation Results and Measurements

As special case it is calculated the reflection factor of Sierpinski gasket antenna with a side length 10cm. The feeding mechanism is carried out by a wire with radius of 1 mm and length of 1cm. In this work it is observed Sierpinski gasket antenna up to third iteration (as shown Figure 5). The first iteration of Sierpinske gasket is a triangle with same side length of 10cm. The generation of the next is by scaling down the side length with factor 0.5 and arranging three such triangles.

In hybrid method SIEM+UTD, just direct, single reflection on the ground and single diffractions on the four edges of the ground are taken into account. Corner diffractions on the tips of the ground and double and more diffraction are neglected. In hybrid method SIEM+PO, any visibility proof in this work do not performed, because we have just one PO structure, so that overall part of the ground is lit by the monopole.

4.1. Comparison between different methods

In this sub section, it is observed the calculation of the antennas by different methods. Figure 8, Figure 9 and Figure 10 show reflection factor of Sierpinki gasket antenna of first, second and third iteration, respectively. In all figures, the four curves as results of different approaches are shown. The solid line is the result for Sierpinksi gasket antenna dipole (left side of Figure 5), or it can be modeled by metallic ground of infinite extent, the calculation is carried out by pure SIEM. The results clear multiband characteristics of the Sierpinksi gasket antennas can be shown. It is found that minima at about 0.5GHz, 1.8GHz and 3.4GHz.
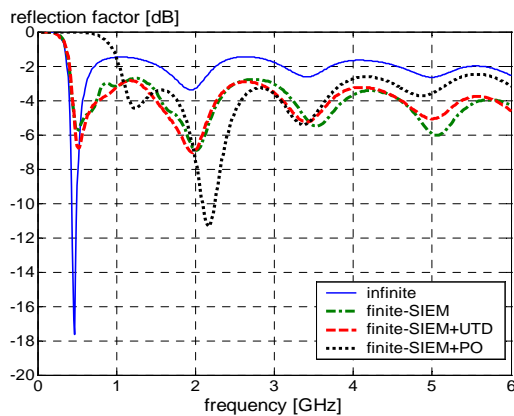

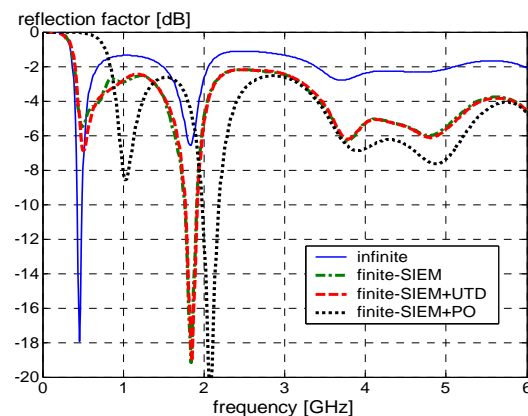Figure 8 Reflection factor of Sierpinski gasket antenna of first iteration

Figure 9 Reflection factor of Sierpinski gasket antenna of second iteration

In this part, the ground with finite size (40x40cm) is also observed and calculated with pure SIEM (dot-dashed line), hybrid method SIEM+UTD (dashed line) and hybrid method SIEM+PO (dotted line). It is shown in all iteration that the finite ground causes almost disappearance of the minimum at 0.5GHz, on the other hand, the minima at 1.8GHz and 3.4GHz are stronger. The hybrid method SIEM+PO (dotted line) shows not so good agreement with the finite SIEM (dot-dashed line) in both first iterations, but shows very well similarity for the structure of third iteration.

In SIEM+PO, the current of the the finite ground, especially near the edges, is just an approximation derived from the incident wave. In some instances, the current can be inaccurate and delivers wrong feedback to the SIEM structures. In all iterations shown in Figure 8, Figure 9 and Figure 10, the hybrid method SIEM+UTD (dashed lines) delivers very good results compared to the SIEM (dot-dashed line). The only small deviations between both methods are shown.
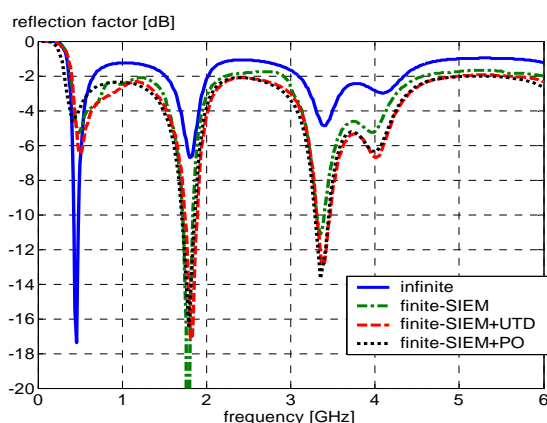
reflection factor [dB]

Figure 10 Reflection factor of Sierpinski gasket antenna of third iteration calculated

Table 1. Memory requirement (RAM) and computational time pro frequency.

Case	Memory req.	Comp.time/ f
1:infinite	8.229 MB	3.97 s
1:finite	416.58 MB	277.47 s
1:finite +PO	33.064 MB	39.47 s
1:finite +UTD	0.432 MB	3.34 s
2:infinite	1.018 MB	0.5 s
2:finite	413.99 MB	285.0 s
2:finite +PO	28.72 MB	27.22 s
2:finite +UTD	0.358 MB	2.64 s
3:infinite	0.944 MB	0.625 s
3:finite	413.77 MB	282.56 s
3:finite +PO	27.41 MB	31.25 s
3:finite +UTD	0.339 MB	2.09 s

Table 1 gives information on the required computer memory (RAM) and the computational time for every frequency point. The hybrid method SIEM+UTD offers indeed the most economical alternative in the calculation. The memory requirement for higher iteration is smaller than for lower, because more holes in higher iteration is haved, so that less element to be considered.

The calculation is carried out in a dual core processor (P8400 2.26GHz) with operating system Microsoft Windows XP Professional Service Pack 2 (Build 2600), Version 5.1.2600.

4.2. Effects of finite grounds

Moreover it is also calculated ground with different dimensions, the large ones as shown in previous subsection (40x40cm) and smaller ground (20x20cm). The calculation is done with SIEM+UTD hybrid method. Comparison between Figure 11 and Figure 12 show that the minima at 1.8GHz and at 3.4GHz become weaker that means the performance of the multiband antennas goes worse.

It is clear to understand, if the dimension of the ground is smaller, the ground as model of the symmetry plane becomes worse, the best model of the antenna, i.e. the Sierpinski gasket dipole cannot be modeled effectively with this condition.

4.2. Measurements

In this work it is built the prototype for all three iterations. The photograph of the Sierpinksi gasket monopoles on finite ground are depicted in Figure 13. The brass of 1 mm thick for the antena and for the ground and a 50ohm N-connectors for feeding purposes are used.

The measurement of the reflection factor of the antenna by making use of a vector network is analyzed by Anritsu MS2026A. Figure 14, Figure 15 and Figure 16 show the comparison between simulation (Figure 12) and measurements. It is shown here, as predicted

by computer calculation; the minimum at 0.5GHz almost disappears. Probably, due to the small frequency, the wavelength at the first minimum is larger than the dimension of the ground, so that the ground has less effect to produce any minimum at this frequency.
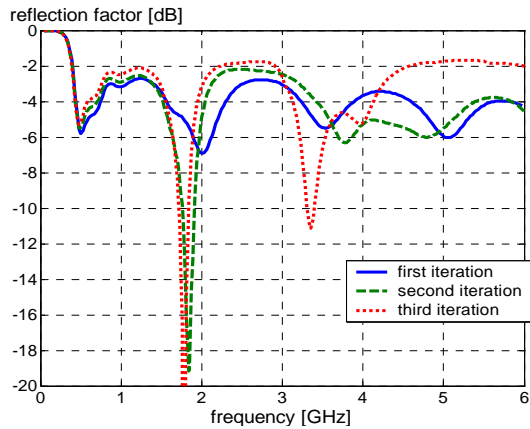
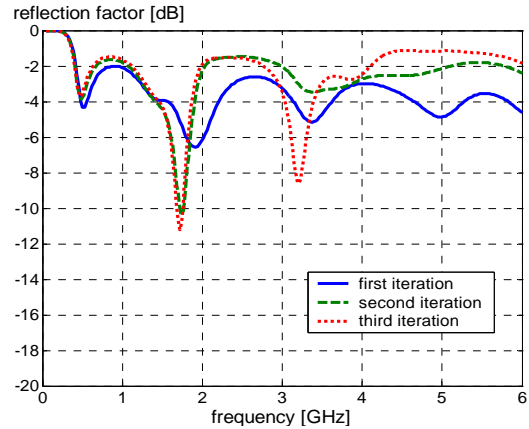Figure 11 Reflection factor of Sierpinski gasket antenna for larger ground (40x40cm)

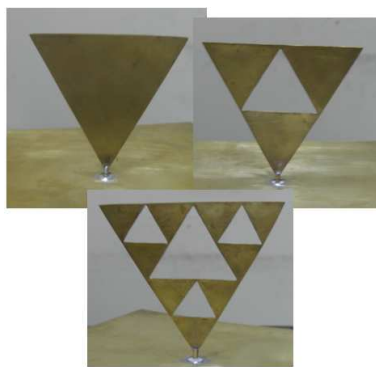Figure 12 Reflection factor of Sierpinski gasket antenna for smaller ground (20x20cm)
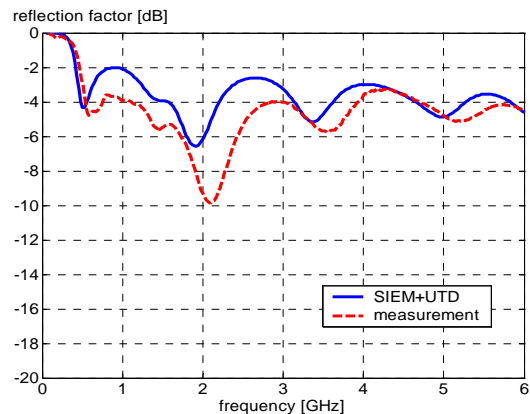
Figure 13 Photograph of the built protoypes

Figure 14 Comparison between simulation and measurement with ground (20 20cm), case iteration 1
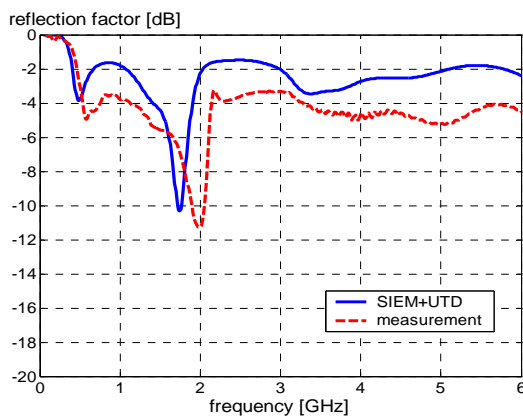
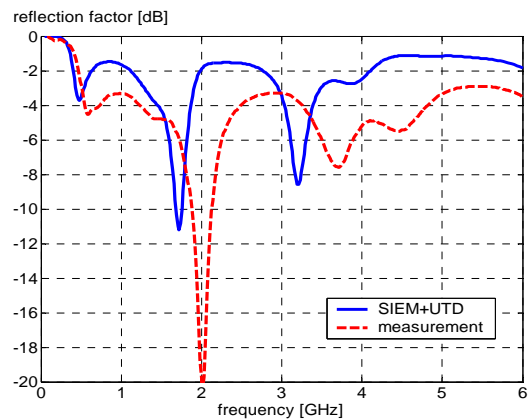Figure 15 Comparison between simulation and measurement with ground (20x20cm), case iteration 2

Figure 16 Comparison between simulation and measurement with ground (20x20cm), case iteration 3

The second minimum, predicted is about 1.8GHz, is shifted to about 2.0GHz. It is not clear what the cause of this shifting is, probably due to the inaccuracy during the fabrication of the antennas or due to the antenna thickness of 1 mm, which was not considered in the simulation. Interestingly it is found for the third iteration third minimum at about 3.6GHz, and fourth minimum at about 4.4GHz, both also shifted to higher frequencies. Shifting to higher frequencies means the actual structures seem shorter than the simulated ones.

5. Conclusion

The Sierpinski gasket antennas observed in this work show the multiband characteristics. All numerical approachs are able to predict this character. The measurements deliver also the similar results. Numerical approach shows, that substituting the dipole by monopole with finite ground leads to disappearance of one of the minimums, i.e. at 0.5GHz. This condition is also verified by the measurements.

Hybrid method SIEM+UTD introduced is a very good alternative because the method gives almost same results as delivered by the exact method SIEM. The memory requirements for examples in this work are less than 1 MB and the computational time shorter than 5 seconds pro frequency point. This small computational effort can lead to more exploration of the structures to get same optimized condition by varying, for example one of the dimensions of the antenna.

References

[1] Puente-Baliarda C, Romeu J, Pous R, Cardama A. On the Behavior of the Sierpinski Multiband Fractal Antenna. *IEEE Transc. On Antennas Propagation.* 1998; 15(4):517-524.
[2] Song CTP, Hall PS, Ghafouri-Shiraz H. Perturbed Sierpinski Multiband Fractal Antenna with Improve Feeding Technique. *IEEE Transc. On Antennas Propagation.* 2003; 51(5):1011-1017.
[3] Krzysztofik WJ. Modified Sierpinski Fractal Monopole for ISM-Bands Handset Applications. *IEEE Transc. On Antennas Propagation.* 2009; 57(3): 606-615.
[4] Puente-Baliarda C. An Iterative Model for Fractal Antennas: Application to the Sierpinski Gasket Antenna. *IEEE Transc. On Antennas Propagation.* 2000; 48(5): 713-719.
[5] Hwang KC, A Modified Sierpinski Fractal Antenna for Multiband Application. *IEEE Antennas & Wireless Propagation Letters.* 2007; 6(1): 357-360.
[6] Best SR. A Multiband Conical Monopole Antenna Derived from a Modified Sierpinski Gasket. *IEEE Antennas & Wireless Propagation Letters.* 2003; 2(1): 205-207.
[7] Alaydrus M. *Analysis of Three Dimensional Sierpinski Gasket Antennas,* Indonesia-Malaysia Microwave Antenna Conference. Depok. 2010. 101-104.
[8] Sadiku MNO. Numerical Techniques in Electromagnetics with Matlab. Third Edition. Boca Raton: CRC Press. 2009.
[9] Morita N, Kumagai N, Mautz JR. Integral Equation Methods for Electromagnetics. Boston: Artech House Publishers. 1991.
[10] Peterson AF, Ray SL, Mittra R. Computational Methods for Electromagnetics. New Jersey: IEEE Press. 1997.
[11] McNamara DA, Pistorius CWI, Malherbe JAG, Introduction to the Uniform Theory of Diffraction. Massachusetts: Artech House Publishers. 1990.
[12] Knott EF, Shaeffer JF, Tuley MT. Radar cross section. Second Edition. Raleigh: SciTech Publishing. 2004
[13] Djordjevic M, Notaros BM. Higher Order Hybrid Method of Moments-Physical Optics Modeling Technique for Radiation and Scattering from Large Perfectly Conducting Surfaces. *IEEE Transc. On Antennas Propagation.* 2005; 53(2):800-813.
[14] Alaydrus M, Hansen V, Eibert TF. Hybrid[2]: Combining the Three-Dimensional Hybrid Finite-Element-Boundary Integral Technique for Planar Multilayered Media with the Uniform Geometrical Theory of Diffraction, *IEEE Transactions Antennas Propagation.* 2002; 50(1): 67-74.
[15] Alaydrus M, Hansen V. *Higher Order Mechanisms and Coupling in the Hybrid[2] Method for Calculating Near and Far Fields of Complex Composite Radiating Structures.* Antennas and Propagation International Symposium. Utah. 2000. 1: 480-483.